An integrated level set model with active contours for image segmentation

Hui Wang[1] and Yingqiong Du[2]

[1] School of Mathematics and Physics, Anshun University, Anshun, Guizhou 561000, China

[2] School of Resources and Environment Project, Anshun University, Anshun, Guizhou 561000, China

Abstract

By incorporating the merits of the geodesic active contour (GAC) model and the Chan-Vese (C-V) model, an integrated level set model with active contours is proposed, which can comprehensively utilize edge information and statistic region information of the image. First a flexible edge detection function is designed, which inspired by the idea of total variation (TV) norm. Then a new speed function based on the statistic region information in and out of active contours is constructed, and correspondingly a new level set formulation is obtained. Finally, the model of this paper is proposed which is made up of distance regularization level set evolution (DRLSE) term, partial GAC model and the new level set formulation. The proposed model can eliminate the need of costly re-initialization procedure for traditional level set methods. Some experiments of synthetic, real-world images are used to test the validity of the proposed model.

Keywords: Image Segmentation, Active Contour Model, Level Set Method, Edge Detection Function, Speed Function.

1. Introduction

Image segmentation is a fundamental and important problem in image processing, analysis and computer vision. It mainly aims to subdivide an image into a series of non-intersected parts and extract interesting objects. In recent years, active contour models [1-3] have been increasingly and widely used in the field of image segmentation. These models mainly need to initialize a close curve called curve of evolution and drive it evolution to realize image segmentation. Active contour models are classified as parametric active contour models [1][4] and geometric active models [3][5-12]. Parametric active contour models depend on parametric equations to represent evolution curves explicitly, and geometric active contour models represent evolution curves implicitly by using the level set method. As a kind of numerical technique for tracking the interfaces and shapes [9], the level set method has been applied to image segmentation in the last score years [2][6-8][13-16], In the level set method, curves or surfaces are represented as zero level set

of a higher dimensional level set function and image segmentation problem can be connected to corresponding mathematics theories, such as partial differential equations (PDEs), calculus of variations [17], geometry and optimization and so on [18-21]. The general form [9] of level set formulation is defined as follows

$$\frac{\partial \phi}{\partial t} = F |\nabla \phi| \qquad (1)$$

where $\phi : (t, \cdot) \rightarrow R$ is the level set function, and F is called speed function. The most important advantage of the level set method is easy to represent contours or surfaces and able to handle topological changes such as splitting and merging in a natural way. Usually image segmentation models based on the level set method are mainly classified into two classes: edge-based models [2-3][7-8][13][22] and region-based models [6][14][23-26]. Edge-based models use edge information to attract the active contours toward the object boundaries and stop there. These models are mainly used by introducing edge detection function comprising image gradient to stop the evolution contours on the boundaries of the desired objects. GAC model [2-3] is a classical and famous example of this class. This kind of models is sensitive to initial conditions and usually with serious boundary leakage problems. Region-based models aim to identify each region of interest by using a certain region descriptor to guide motion of active contours to realize image segmentation. Comparing with the edge-based models, region-based models have an explicit advantage to utilize the statistical region information inside and outside contours to control the level set evolution. The region-based models are less sensitive to noise and have better effectiveness on those images with weak edges or blurred edges. Some typical examples of this kind are piecewise constant models [6], piecewise smooth models [23-24] which are based on the work of Mumford and Shah [27]. In the traditional level set method, level set function needs re-initialization [28] as a numerical remedy to restore the regularity and maintain the stability. Re-initialization is performed by periodically stopping the evolution and reshaping the

degraded level set function as signed distance function, which is realized by solving the following PDE [11]

$$\frac{\partial \psi}{\partial t} = sign(\phi)\big(1 - |\nabla \psi|\big) \qquad (2)$$

where ϕ is the level set function to be re-initialized, and the solution ψ is the new level set function, and $sign(\cdot)$ is common sign function. The process of re-initialization is complicated and time-consuming in spite of being widely used. To overcome this problem, a general variational level set formulation [15] with a distance regularization term named distance regularization level set evolution (DRLSE) method is proposed. The distance regularization term is defined with a potential function which can force the gradient magnitude of the level set function to converge to those minimum points so as to maintain the desired shape of level set function. The DRLSE method introduces a double-well potential for the distance regularization term and completely eliminates the need for re-initialization and avoids the undesirable side effect introduced by the penalty term in [7].

In the existing image segmentation models, most of them are based on edge information or statistical region information. Besides, there are some methods [29-31] which integrate both of them. In fact, it is difficult to find a fit weight to balance them, especially, which is irreconcilable in some cases. In this paper, an integrated level set model with active contours based on edge information and statistical region information is proposed, which incorporates the merits of the GAC model [2-3], the C-V model [6] and the DRLSE method. First a new edge detection function based on the idea of TV norm [32-33] is designed. Second a new speed function based on the statistical region information is constructed. Finally, the model of this paper is proposed. The proposed model integrates edge information and statistical region information and the realization of numerical scheme is simple. Furthermore, considering the proposed model is PDE-based, a Gaussian function is used to filter the level set function [34].

The outline of this paper is organized as follows. In section 2, a review of the GAC model, the C-V model and the DRLSE method is provided. In section 3, we design a edge detection function, and construct a speed function and obtain a new level set formulation. Then the model of this paper is proposed. In section 4, in comparison with other image segmentation models [3][6][35], some experimental results are presented. Finally, we end this paper with a brief conclusion in section 5.

2. Background

2.1 The GAC model

The GAC model [2-3] is derived from the development of the snake model [1], which based on the edge information of the image is defined by the following problem

$$\min_{C} \left\{ E_{GAC}(C) = \int_{0}^{L(C)} g\big(|\nabla I(C(s))|\big) ds \right\} \qquad (3)$$

where ds is the Euclidean element of length, and $L(C)$ is the length of the closed curve C, and g is the edge detection function, and I is the original image defined by $I : \Omega \to R$. In calculus of variations, a standard method is used to minimize (3) and accordingly the gradient flow equation is obtained as follows:

$$\frac{\partial C}{\partial t} = \big(\kappa g - \langle \nabla g, N \rangle\big) N \qquad (4)$$

where κ and N are represented the curvature and the normal of the curve C respectively. In the level set method, the evolution (4) can be represented as the level set formulation

$$\frac{\partial \phi}{\partial t} = g\, div\left(\frac{\nabla \phi}{|\nabla \phi|}\right)|\nabla \phi| + \nabla g \cdot \nabla \phi \qquad (5)$$

where ϕ is the level set function embedded in the active contour C and $div(\cdot)$ is the divergence operator. The numerical schemes of the level set formulation (5) are based on hyperbolic conservation laws [28]. The GAC model is sensitive to the choice of the initial contour and setting an inappropriate initial contour may lead to slow convergence and achieve an unsatisfactory result. Because of depending on the edge information of the image, the GAC model is sensitive to noise. In particular, the primal GAC model is fail in some special examples with hollow region. Generally a constant term α called balloon force is added to speed up the contour shrinking or expanding, and consequently (5) can be represented as

$$\frac{\partial \phi}{\partial t} = g\left(div\left(\frac{\nabla \phi}{|\nabla \phi|}\right) + \alpha \right)|\nabla \phi| + \nabla g \cdot \nabla \phi \qquad (6)$$

However, the choice of α is not easy in the experiment of image segmentation.

2.2 The C-V model

As a special case of Mumford-Shah functional problem, the C-V model [6] proposed by Chan and Vese firstly is one of the most popular image segmentation models based on the statistic region information. It is realized by minimizing the following energy functional

$$E(C, c_1, c_2) = \mu \cdot |C| + \lambda_1 \int_{inside(C)} (I(x,y) - c_1)^2 \, dxdy$$
$$+ \lambda_2 \int_{outside(C)} (I(x,y) - c_2)^2 \, dxdy$$
$$(7)$$

where $\mu \geq 0$, $\lambda_1 \geq 0$ and $\lambda_2 \geq 0$ are fixed parameters. The first term of energy functional (7) is the length restraint term of contour C and the combination of the second term and the third term is called fitting term based on statistic region information of inside and outside contour C. In the calculus of variations and the level set method, we first fix c_1 and c_2 and introduce Heaviside function H and Dirac function δ to minimize energy functional (7), and then we obtain the corresponding level set formulation

$$\frac{\partial \phi}{\partial t} = \mu \cdot \delta(\phi) div\left(\frac{\nabla \phi}{|\nabla \phi|} \right)$$
$$- \delta(\phi)\left[\lambda_1 (I(x,y) - c_1)^2 - \lambda_2 (I(x,y) - c_2)^2 \right]$$
$$(8)$$

Next we use the same minimization method to fix the level set function ϕ, and obtain c_1 and c_2 defined as follows

$$\begin{cases} c_1(\phi) = \dfrac{\int_\Omega I(x,y) H(\phi(x,y)) dxdy}{\int_\Omega H(\phi(x,y)) dxdy} \\ c_2(\phi) = \dfrac{\int_\Omega I(x,y)(1 - H(\phi(x,y))) dxdy}{\int_\Omega (1 - H(\phi(x,y))) dxdy} \end{cases} \quad (9)$$

The C-V model is very effective in images with weak edges even without edges. In fact, it is a non-convex problem. In [6], Chan and Vese use a finite difference implicit scheme to discretize (8) and solve it by using the iterative method. One of the disadvantages of the C-V model is that it cannot achieve ideal effectiveness in multi-objects images with different intensities.

2.2 DRLSE

As a general variational level set formulation, the DRLSE method firstly proposed in [15] is used to eliminate the re-initialization of traditional level set methods and maintain a desired shape of the level set function. First we review the level set regularization term $R_p(\phi)$ defined by Li *et al.* in [15] as follows

$$R_p(\phi) = \int_\Omega p(|\nabla \phi|) dxdy \quad (10)$$

where p is called potential function. In calculus of variations, it is easy to give the gradient flow equation

$$\frac{\partial \phi}{\partial t} = div\left(d_p(|\nabla \phi|)\nabla \phi \right) \quad (11)$$

where the function d_p defined by

$$d_p(s) = \frac{p'(s)}{s} \quad (12)$$

The double-well potential function $p(s)$ is defined by

$$p(s) = \begin{cases} \dfrac{1}{(2\pi)^2}(1 - \cos(2\pi s)), & s < 1 \\ \dfrac{1}{2}(s-1)^2, & s \geq 1 \end{cases} \quad (13)$$

The first derivative of $p(s)$ is given by

$$p'(s) = \begin{cases} \dfrac{1}{2\pi}\sin(2\pi s), & s < 1 \\ s - 1, & s \geq 1 \end{cases} \quad (14)$$

From (12) and (14), we obtain

$$d_p(|\nabla \phi|) = \begin{cases} \dfrac{\sin(2\pi|\nabla \phi|)}{2\pi|\nabla \phi|}, & |\nabla \phi| < 1 \\ 1 - \dfrac{1}{|\nabla \phi|}, & |\nabla \phi| \geq 1 \end{cases} \quad (15)$$

Then (11) can be expressed as

$$\frac{\partial \phi}{\partial t} = \begin{cases} div\left(\dfrac{\sin(2\pi|\nabla \phi|)}{2\pi|\nabla \phi|}\nabla \phi \right), & |\nabla \phi| < 1 \\ div\left(\left(1 - \dfrac{1}{|\nabla \phi|}\right)\nabla \phi \right), & |\nabla \phi| \geq 1 \end{cases} \quad (16)$$

When $|\nabla \phi| \geq 1$, it is the same discussion and analysis as in [7].

3. Description of the proposed model

3.1 Designing of the edge detection function

Edge is one of the most important information of the image and edge detection is primary work in image segmentation and recognition [30]. To simplify, we set the image as 2-dimensional matrices of size $M \times N$. Generally gradient information is used to design the edge detection function in image segmentation methods, and a general choice is given by

$$g_1 = \frac{1}{1 + |\nabla I|^2} \quad (17)$$

where $|\nabla I|$ is the gradient module of the image I.

For convenience, we analyze the discrete form of $|\nabla I|$. In the total variation (TV) regularization criterion [32][36], the energy functional is defined by

$$TV(I) = \int_{\Omega} \|\nabla I\| dxdy \qquad (18)$$

where ∇I is a vector given by

$$\nabla I = \left(\nabla_x I(i,j), \nabla_y I(i,j)\right)$$

with

$$\nabla_x I(i,j) = \begin{cases} I_{i+1,j} - I_{i,j}, i < M \\ 0, i = M \end{cases}$$

$$\nabla_y I(i,j) = \begin{cases} I_{i,j+1} - I_{i,j}, j < N \\ 0, j = N \end{cases}$$

In practical computation, usually, there are two kinds of discrete forms of the energy functional (18). Choosing the 2-norm defines isotropic TV as follows

$$TV(I) = \sum_{1 \le i \le M, 1 \le j \le N} \sqrt{\left(\nabla_x I(i,j)\right)^2 + \left(\nabla_y I(i,j)\right)^2} \quad (19)$$

which means that TV is invariant to rotation, reflection, and changing of position of the image. Correspondingly, choosing the 1-norm defines anisotropic TV as follows

$$TV(I) = \sum_{1 \le i \le M, 1 \le j \le N} \left(\left|\nabla_x I(i,j)\right| + \left|\nabla_y I(i,j)\right|\right) \quad (20)$$

Actually using the anisotropic TV is better to preserve fine detail of edge and texture than the isotropic TV. On the basis of above analysis about 1-norm and 2-norm of TV, we design a new edge detection function from a combination of them as follows

$$g = \frac{1}{1 + (1-\lambda)\|\nabla I\|_1 + \lambda \|\nabla I\|_2^2} \qquad (21)$$

where $\|\nabla I\|_1$ and $\|\nabla I\|_2^2$ are 1-norm and the square of 2-norm, respectively. Here, it is necessary to explain a bit that we choose the square of 2-norm for calculating easily. Further we obtain

$$g = \frac{1}{1 + (1-\lambda)(|\nabla_x I| + |\nabla_y I|) + \lambda((\nabla_x I)^2 + (\nabla_y I)^2)}$$

$$(22)$$

where λ is a fixed parameter. In general, we set $0 \le \lambda \le 1$. When $\lambda = 1$, (22) is equivalent to (17). In other words, (17) is a special case of (22). When $\lambda = 0$, (22) can be represented by the following form

$$g_2 = \frac{1}{1 + |\nabla_x I| + |\nabla_y I|} \qquad (23)$$

To test and compare the similarity and difference of (17), (22) and (23), we design a simple experiment and the results are shown in Fig.1. In the experiment, the result of (17) has a higher contrast, while the result of (23) has a higher capability in anti-noise interference to be better effectiveness on edge and texture preservation. Generally, the combination of 1-norm and 2-norm is used to obtain (22) with the alteration of parameter λ, which is more flexible than (17) and (23), respectively. To obtain good results in images with different characteristics, $\lambda = 1$ is chosen for images with high contrast, and $\lambda = 0$ for images with weak or blurred edges.
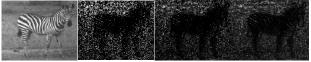

Fig. 1 Comparison of edge detection functions with original image, the results of g_1 in (17), g with $\lambda = 0.5$ in (22) and g_2 in (23) from left to right.

3.2 Construction of the level set speed function

In level set formulation (1), the form of speed function F is very critical in the evolution process of the level set. In practice, how to choose and construct a fit speed function F is one of the major issues. Considering the effectiveness of region-based image segmentation models especially the C-V model, we first give the fitting term of energy functional defined in [6] as

$$\int_{in(C)} \left(I(x,y) - c_1\right)^2 dxdy + \int_{out(C)} \left(I(x,y) - c_2\right)^2 dxdy$$

$$(24)$$

The Euler-Lagrange equation of this fitting term is as follows

$$\delta(\phi)\left(\left(I(x,y) - c_1\right)^2 - \left(I(x,y) - c_2\right)^2\right) = 0 \quad (25)$$

In a small region near the contour, $\delta(\phi) \ne 0$, then (25) can be compactly written as

$$\left(c_2 - c_1\right)\left(2I(x,y) - (c_1 + c_2)\right) = 0 \qquad (26)$$

That is, the solutions of (26) must be the solutions of (25). Further, (26) can be divided into two parts as follows

$$I(x,y) - \frac{c_1 + c_2}{2} = 0$$

and

$$c_1 - c_2 = 0$$

Therefore two of the optimal solutions of (25) are $I(x,y) = \dfrac{c_1 + c_2}{2}$ and $c_1 = c_2$. In fact, calculating all the solutions of (25) for a small region near the contour is very difficult in most cases, so we can choose appropriate

contours to let $\left| I(x,y) - \dfrac{c_1 + c_2}{2} \right| \to 0$ or $|c_1 - c_2| \to 0$.

When $\left| I(x,y) - \dfrac{c_1 + c_2}{2} \right| \to 0$, $|c_1 - c_2| \to \alpha_0$, where

α_0 is a constant. Considering the basis on the above analysis of the fitting term, we construct a new speed function

$$F = \frac{I(x,y) - \dfrac{c_1 + c_2}{2}}{|c_1 - c_2|} \qquad (27)$$

Thus (1) can be rewritten as follows

$$\frac{\partial \phi}{\partial t} = \left(\frac{I(x,y) - \dfrac{c_1 + c_2}{2}}{|c_1 - c_2|} \right) |\nabla \phi| \qquad (28)$$

Using (28), with the process of updating the level set function, its zero level set contour keep on changing, and no matter where the initial contour is, $I(x,y) - \dfrac{c_1 + c_2}{2}$ always become smaller and smaller. Meanwhile, the change of $|c_1 - c_2|$ is uncertain in the beginning and gradually stable, and then nears a constant after some iterations. For the convenience, we introduce a positive constant β into (28), and then a new level set formulation is proposed as follows

$$\frac{\partial \phi}{\partial t} = \beta \left(\frac{I(x,y) - \dfrac{c_1 + c_2}{2}}{|c_1 - c_2|} \right) |\nabla \phi| \qquad (29)$$

where c_1 and c_2 are given by (9). To illustrate the effectiveness of the level set formulation (29), we apply it to some synthetic and real-world images in Fig. 2. The initial contours and the results of 80 iterations with $\beta = 1$ are showed in the first column and the second column, respectively. The changing curves of maximum absolute value of the speed function F with the increasing iterations are showed in the third column. The curves illustrate that the maximum absolute value of the speed function gradually tends to zero with updating the level set function, which means that the evolution speed of the level set is more and more slow until convergence.
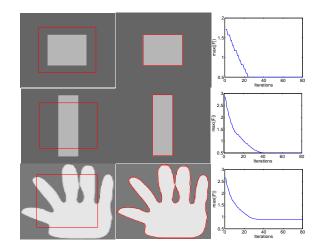

Fig. 2 Results and curves. The first column: initial contours. The second column: results of (29) with $\beta = 1$ in 80 iterations. The third column: changing curves of maximum absolute value of speed function ($\max(|F|)$) in (27) with the increasing iterations.

3.3 The proposed model and implementation

On the basis of the introduction and discussion of the DRLSE method, the designing of the edge detection function and the construction of the level set speed function, in order to make full use of edge information and region information of image and inherit the advantages of the GAC model and the C-V model, we propose an integrated level set model with active contours as follows

$$\frac{\partial \phi}{\partial t} = \mu \, div\big(d_p(|\nabla \phi|)\nabla \phi\big) + \alpha g \, div\left(\frac{\nabla \phi}{|\nabla \phi|}\right)|\nabla \phi| + \beta F |\nabla \phi| \qquad (30)$$

where $d_p(|\nabla \phi|)$ is given by (15), and g is the new edge detection function designed by (22), and F is defined by (27), and μ, α, β are nonnegative parameters.

The proposed model applies the form of integration [30] to achieve synthesis of the DRLSE method, partial GAC model and the new level set formulation in (29). The first term is the introduction of the DRLSE method to eliminate the re-initialization and maintain a desired shape of the level set function. In some extent, it can satisfy stability and accuracy requirement to use relatively large time step in finite difference scheme. The second term is derived from partial GAC model which contains the new edge detection function in (22) to improve the flexibility in image with different kinds of edges and textures. From the point of another respect, we can find that the second term is similar to weighted mean curvature motion equation and the weight function is the edge detection function given in

(22). The third term is given by (29) which contains statistic region information in and out of active contours.

In application of the proposed model, the parameters μ, α and β are very important for performance. The parameter μ is used to control the weight of regularization level, and in most cases it should be small as discussed in [15]. The parameter α is used to control the weight of the proposed model relying on edge information and similarly the parameter β is used to control the weight of the proposed model relying on statistic region information. The ratio between α and β is very critical. Fixing β and choosing a large α signify that the weight of relying on the edge information is large. Correspondingly, fixing α and choosing a large β signify that the weight of relying on the statistic region information is large. For noise free images with clear boundaries, choosing a large α and a small β is suitable to accelerate the iterative convergence rate greatly. While for those images with noise and weak or blurred boundaries choosing a small α and a large β is appropriate to avoid edge leakage and over-segmentation.

Generally, there are three kinds of discrete numerical schemes for solving the proposed model, which are forward difference, backward difference and center difference. In this paper, we use the simple explicit finite forward difference method to discretize (30). Usually, we set Δt as time step and h as space step, and then $\phi_{i,j}^n = \phi(n\Delta t, x_i, y_j)$, where $(x_i, y_j) = (ih, jh)$. In the experiments of digital images, we often choose $h = 1$ in order to calculate conveniently. Then the discrete form of the proposed model is given by

$$\frac{\phi_{i,j}^{k+1} - \phi_{i,j}^{k}}{\Delta t} = L(\phi_{i,j}^{k}) \qquad (31)$$

where the forward difference is used to approximate the left part $\dfrac{\partial \phi}{\partial t}$ and $L(\phi_{i,j}^{k})$ is the approximation of the right part in (30). Based on the introduction of the DRLSE method [15], a simple initialization form of the level set function is used in the proposed model as follows

$$\phi_0(x, y) = \begin{cases} c, (x, y) \in \Omega_0 \\ -c, (x, y) \in \Omega - \Omega_0 \end{cases} \qquad (32)$$

where $c > 0$ is a constant, and Ω_0 is the domain of image inside of the contour C and Ω is the domain of the image. Besides, we can also choose a traditional initialization form defined by a sign distance function

$$\phi_0(x, y) = -\sqrt{(x - x_0)^2 + (y - y_0)^2} + r \qquad (33)$$

where $r > 0$ is a constant.

with updating the level set function, the level set may become less and less smooth, so a Gaussian filter is introduced to smooth it [35][37], which is desirable and meaningful for PDE-based level set models. Then we give the principal steps of algorithm on the basis of the proposed model in the following

1. Initial parameters: μ, α, β, λ, σ.
2. Compute edge detection function g by (22).
3. Initialization level set function: $n = 1$, $\phi^1 = \phi_0$.
4. Compute $c_1(\phi^n)$ and $c_2(\phi^n)$ by (9).
5. Update level set function ϕ^{n+1} by solving (30).
6. Gaussian filter: $\phi^{n+1} = \phi^{n+1} * G_\sigma$, where G_σ is a Gaussian function.
7. Check whether the solution is stationary. If not, $n = n + 1$ and go to step 4.

Remark 1. In step 6, we use a Gaussian filter G_σ with standard deviation σ to smooth the level set function. The parameter σ is important and should be chosen appropriately and usually it ranges from 0.8 to 1.5.

4. Experimental results and analysis

The experiments of the proposed model mainly involve a variety of synthetic and real-world images. All the experiments are implemented in Matlab 7.0 and the experimental device is Inter Pentium(R) CPU 3.00 GHz with 1 GB of RAM. The partial basic initial parameters are set as $\mu = 0.04$, $\sigma = 1.5$ and $K = 5$, where K is width of the Gaussian kernel mask in the step 6 of our algorithm. In the following experiments, we set the time step as $\Delta t = 0.5$. In order to show the validity of the proposed model, we compare it with the GAC model and the C-V model, and the method in [35].

In Fig. 3, the GAC model and the proposed model are compared to segmenting the image with a little noise and weak and blurred boundaries. The initial level set function is set as a signed distance function $\phi_0(x, y) = -\sqrt{(x - 42)^2 + (y - 42)^2} + 35$. The left image is the initial contour and the middle image is the result of the GAC model in which we do re-initialization every 10 iterations. The result of the GAC model shows that the performance is not perfect with over-segmentation and false detection in some region. The proposed model detects the boundaries accurately in the right image. The

IJCSI International Journal of Computer Science Issues, Volume 17, Issue 1, January 2020
ISSN (Print): 1694-0814 | ISSN (Online): 1694-0784
www.IJCSI.org

https://doi.org/10.5281/zenodo.3987094

7

results of comparison shows the proposed model is less sensitive to noise and has a better performance on those images with weak boundaries. The proposed model takes only 0.55 s in 10 iterations while the GAC model takes 115.5 s in 2000 iterations.

Fig. 3 Results for a noisy image with weak and blurred boundaries. The left image is the initial contour. The middle image is the result of the GAC model where $\alpha = 0.5$. The right image is the result of the proposed model where $\lambda = 1$, $\alpha = 1$ and $\beta = 10$.

In Fig. 4, we compare the effectiveness of the C-V model with the proposed model. The first column is two different kinds of initial contours. The second column is the results of the C-V model which cannot detect all the objects for it relying on the initialization of contours. The third column is the results of the proposed model which detects all the three objects completely. The results of comparison show that the proposed model has global segmentation property without relying on the initialization of the contour.
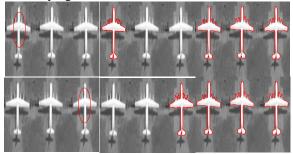

Fig. 4 Results of comparing the C-V model with the proposed model. The first column: initial contours. The second column: results of the C-V model where $\mu = 0.1 \times 255^2$, $\lambda_1 = \lambda_2 = 1$. The third column: results of the proposed model where $\lambda = 1$, $\alpha = 1$, $\beta = 10$.

In Fig. 5, we compare the proposed model with the C-V model on the images with intensive noise or blurred boundaries. The size of images are 101×99 pixels and 105×108 pixels respectively. The first column is initial contours. The second column and the third column are the results of the C-V model and the proposed model, respectively. The C-V model takes 4.75 s in the first row and 8.5 s in the second row and correspondingly the proposed model takes 2.65 s and 2.57 s. From the results of comparison we can see that all the objects are detected accurately, which show that the proposed model is robust

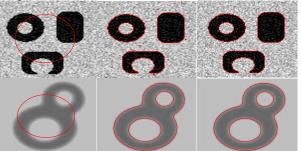and have a similar performance as the C-V model for these images with intensive noise or blurred boundaries.

Fig. 5 Comparison of the C-V model and the proposed model for images with intensive noise in the first row and blurred boundaries in the second row. The first column is initial contours. The second column and the third column are the results of the C-V model and the proposed model. The parameters of the C-V model are $\mu = 0.1 \times 255^2$, $\lambda_1 = \lambda_2 = 1$ in the first row and $\mu = 0.01 \times 255^2$, $\lambda_1 = \lambda_2 = 1$ in the second row. The parameters of the proposed model are $\lambda = 1$, $\alpha = 1$, $\beta = 10$.

In Fig. 6, we show the similarities and differences by setting different values of the parameters λ in (22) in texture image segmentation. The first column is initial contours. The second column is the results of the proposed model in which we set the parameter $\lambda = 1$, where partial boundaries are missed. Correspondingly in the third column we set the parameter $\lambda = 0$ and most boundaries are detected. From the comparison we can see that the results in the third column are a little better than the results in the second column. The results show that when $\lambda = 0$ the performance of the proposed model is better than $\lambda = 1$ on the edge detection of texture images.
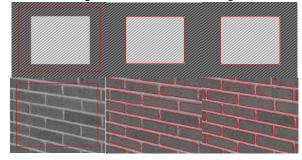

Fig. 6 Comparison of the proposed model with different parameter setting in the edge detection function. The first column: initial contours. The second column: results with $\lambda = 1$. The third column: results with $\lambda = 0$. The parameters of the first row: $\alpha = 1$, $\beta = 2$. The parameters of the second row: $\alpha = 1$, $\beta = 10$.

In Fig. 7, we apply the proposed model in magnetic resonance images in the first row and the second row and an ultrasound image in the third row. The first column is initial contours. The second column is the results of 10 iterations and the third column is the final results in which almost all boundaries are detected clearly.
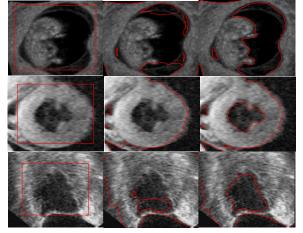

Fig. 7 Results of the proposed model with $\lambda = 0.5$, $\alpha = 1$, $\beta = 5$. The first column: initial contours. The second column: results of 10 iterations. The third column: final results.

A new formulation and level set method named selective binary and Gaussian filtering regularized level set (SBGFRLS) method is proposed in [35], which utilizes the statistic region information and obtains a signed pressure force function for driving the level set evolution. The level set formulation of the SBGFRLS method is given by

$$\frac{\partial \phi}{\partial t} = spf(I(x)) \cdot \alpha |\nabla \phi| \qquad (34)$$

where $spf(I(x))$ is called signed pressure force function, and $\alpha > 0$ is a constant. However, comparing with the SBGFRLS method, the proposed model is more general. In the experiments of Fig. 8, we compare the SBGFRLS method with the proposed model in a natural image and two medical images. The first row is a natural image. The second row is a magnetic resonance image and the third row is an ultrasound image. From the comparison results we can see that the proposed model can obtain similar performance as the SBGFRLS method. In Fig. 9, we use the SBGFRLS method and the proposed model in synthetical images with which the background intensity is higher than the objects. As the experiments in Fig. 8, we obtain similar results, especially that the proposed model performs better in edge detection than the SBGFRLS method.
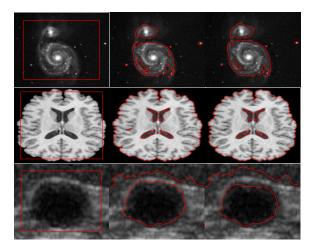

Fig. 8 Comparison of the SBGFRLS method in [35] and the proposed model. The first column: initial contours. The second column: results of the SBGFRLS method. The third column: results of the proposed model. The parameter of the SBGFRLS method is $\alpha = 20$ in the first row and the second row, and $\alpha = 2.5$ in the third row. The parameters of the proposed model are $\lambda = 0.5$, $\alpha = 1$, $\beta = 10$ in the first row and the second row, and $\lambda = 0.5$, $\alpha = 1$, $\beta = 2.5$ in the third row.
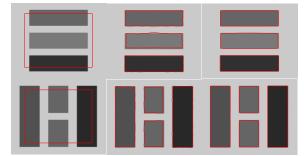

Fig. 9 Comparison of the SBGFRLS method and the proposed model. The first column: initial contours. The second column: results of the SBGFRLS method with $\alpha = 10$. The third column: results of the proposed model with $\lambda = 0$, $\alpha = 1$, $\beta = 10$.

Finally, we test the proposed model in the image with different kinds of intensive noise and the results are showed in Fig. 10. The first column is the initial contour of the original image and the corresponding result. The second column is the initial contour of the image with intensive Gaussian noise and the corresponding result. The mean and the variance of Gaussian noise are 0.1 and 0.01, respectively. The third column is the initial contour of the image with strong Salt and Pepper noise and the corresponding result. The density of Salt and Pepper is 0.1. Unlike the experiments before, we set the time step $\Delta t = 0.2$. The similar results of the second row illustrate that the proposed model is less sensitive to noise.
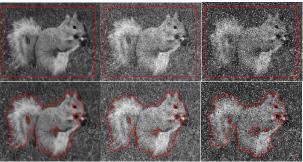
IJCSI
www.IJCSI.org

Fig. 10 The first row is the initial contours and the second row is the results of the proposed model with $\lambda = 0$, $\alpha = 1$, $\beta = 5$.

5. Conclusions

This paper has proposed an integrated level set model with active contours for image segmentation. The proposed model mainly includes three parts: the DRLSE term, the partial GAC model depended on the edge information and the new level set formulation based on the statistic region information of the image. The cores of this paper are designing the edge detection function based on the idea of TV norm, the construction of the speed function of the level set formulation and the presentation of the proposed model. Besides, the proposed model introduced the DRLSE method for eliminating the re-initialization of traditional level set methods and obtains the numerical stability and accuracy of calculation. Furthermore, we employed the Gaussian filter to smooth the level set function. Experimental results show the effectiveness and application of the proposed model.

Acknowledgments

References

[1] M. Kass, A. Witkin, and D. Terzopoulos, "Snakes: active contour models", International journal of computer vision, Vol. 1, No. 4, 1988, pp. 321-331.
[2] V. Caselles, F. Catte, and T. Coll, et al., "A geometric model for active contours in image processing", Numerical mathematics, Vol. 66, No. 1, 1993, pp. 1-31.
[3] V. Caselles, R. Kimmel, and G. sapiro, "Geodesic active contours", International journal of computer vision, Vol. 22, No. 1, 1997, pp. 61-79.
[4] C. Xu, and J. L. Prince, "Snakes, shapes, and gradient vector flow", IEEE transactions on image processing, Vol. 7, No. 3, 1998, pp. 359-369.
[5] D. Adalsteinsson, and J. A. Sethian, "A fast level set method for propagating interfaces", Journal of computational physics, Vol. 118, No. 2, 1995, pp. 269-277.
[6] T. Chan, and L. Vese, "Active contours without edges", IEEE transactions on image processing, Vol. 10, No. 2, 2001, pp. 266-277.
[7] C. Li, C. Xu, and C. Gui, et al., "Level set evolution withgout re-initialization: a new variational formulation", in proceedings of IEEE conference on computer vision and pattern recognition,, 2005, pp. 430-436.
[8] R. Malladi, J. A. Sethian, and B. C. Vemuri, "Shape modeling with front propagation: a level set", IEEE transactions on pattern analysis and machine intelligence, Vol. 17, No. 2, 1995, pp. 158-175.
[9] S. Osher, and J. A. Sethian, "Fronts propagating with curvature-dependent speed: algorithms based on Hamilton-Jacobi formulation", Journal of computational physics, Vol. 79, No. 1, 1988, pp. 12-49.
[10] D. Peng, B. Merrian, and S. Osher, et al., "A PDE based fast local level set method", Journal of computational physics, Vol. 115, No. 2, 1999, pp. 410-438.
[11] M. Sussman, P. Smereka, and S. Osher, "A level set approach for computing solutions to incompressible two-phase flow", Journal of computational physics, Vol. 114, No. 1, 1994, pp. 146-159.
[12] J. S. Suri, K. Liu, and S. Singh, et al., "Shape recovery algorithms using level sets in 2D/3D medical imagery: a state-of-the-art review", IEEE transactions on information technology in biomedicine, Vol. 6, No. 1, 2002, pp. 8-28.
[13] R. Kimmel, A. Amir, and A. Bruckstein, "Finding shortest paths on surfaces using level set propagation", IEEE transactions on pattern analysis and machine intelligence, Vol. 17, No. 6, 1995, pp. 635-640.
[14] C. Li, C. Kao, and J. C. Gore, et al., "Minimization of region-scalable fitting energy for image segmentation", IEEE transactions on image processing, Vol. 17, No. 10, 2008, pp. 1940-1949.
[15] C. Li, C. Xu, and C. Gui, et al., "Distance regularized level set evolution and its application to image segmentation", IEEE transactions on image processing, Vol. 19, No. 12, 2010, pp. 3243-3254.
[16] N. Paragios, R. Deriche, "Geodesic active contours and level sets for detection and tracking of moving objects", IEEE transactions on pattern analysis and machine intelligence, Vol. 22, No. 3, 2000, pp. 266-280.
[17] G. Aubert, and P. Kornprobst, Mathematical problems in image processing: partial differential equations and the calculus of variations, New York: Springer, 2002.
[18] T. F. Chan, S. Esedoglu, and M. Nikolova, "Algorithms for finding global minimizers of image segmentation and denoising models", SIAM journal on applied mathematics, Vol. 66, No. 5, 2006, pp. 1632-1648.
[19] X. Bresson, S. Esedoglu, and P. Vandergheynst, et al., "Fast global minimization of the active contour/snake model", Journal of mathematical imaging and vision, Vol. 28, No. 2, 2007, pp. 151-167.
[20] T. Goldstein, X. Bresson, and S. Osher, "Geometric applications of the split bregman method: segmentation and surface reconstruction", Journal of scientific computing, Vol. 45, No. 1-3, 2010, pp. 272-293.

[21] E. S. Brown, T. F. Chan, and X. Bresson, "Completely convex formulation of the Chan-Vese image segmentation model", International journal of computer vision, Vol. 98, No. 1, 2012, pp. 103-120.

[22] A. Vasilevskiy, and K. Siddiqi, "Flux-maximizing geometric flows", IEEE transactions on pattern analysis and machine intelligence, Vol. 24, No. 12, 2002, pp. 1565-1578.

[23] L. Vese, and T. Chan, "A multiphase level set framework for image segmentation using the Mumford and Shah model", International journal of computer vision, Vol. 50, No. 3, 2002, pp. 271-293

[24] A. Tsai, A. Yezzi, and A. S. Willsky, "Curve evolution implementation of the Mumford-Shah functional for image segmentation, denoising, interpolation, and magnification", IEEE transactions on image processing, Vol. 10, No. 8, 2001, pp. 1169-1186.

[25] R. Ronfard, "Region-based strategies for active contour models", International journal of computer vision, Vol. 13, No. 2, 1994, pp. 229-251.

[26] J. Huang, X. Yang, and Y. Chen, "A fast algorithm for global minimization of maximum likelihood based on ultrasound image segmentation", Inverse Problems and Imaging, Vol. 5, No. 3, 2011, pp. 645-657.

[27] D. Mumford, and J. Shah, "Optimal approximations by piecewise smooth functions and associated variational problems", Communications on pure and applied mathematics, Vol. 42, No. 5, 1989, pp. 577-685.

[28] S. Osher, and R. Fedkiw, Level set methods and dynamic implicit surfaces, New York: Springer, 2002.

[29] J. L. Moigne, and J. C. Tilton, "Refining image segmentation by integration of edge and region data", IEEE transactions on geoscience and remote sensing, Vol. 33, No. 3, 1995, pp. 605-615.

[30] C. S. Sagiv, N. A. Sochen, and Y. Y. Zeevi, "Integrated active contours for texture segmentation", IEEE transactions on image processing, Vol. 15, No. 6, 2006, pp. 1633-1646.

[31] L. Gupta, U. G. Mangai, and S. Das, "Integrating region and edge information for texture segmentation using a modified constraint satisfaction neural network", Image and vision computing, Vol. 26, No. 8, 2008, pp. 1106-1117.

[32] L. Rudin, S. Osher, and E. Fatemi, "Nonlinear total variation based noise removal algorithms", Physica D Nonlinear Phenomena, Vol. 60, No. (1-4), 1992, pp. 259-268.

[33] T. Chan, G. Golub, and P. Mulet, "A nonlinear primal-dual method for total variation-based image restoration", SIAM journal on scientific computing, Vol. 20, No. 6, 1999, pp. 1964-1977.

[34] K. Zhang, L. Zhang, and H. Song, et al., "Re-initialization free level set evolution via reaction diffusion", IEEE transactions on image processing, Vol. 22, No. 1, 2013, pp. 258-271.

[35] K. Zhang, L. Zhang, and H. Song, et al., "Active contours with selective local or global segmentation: a new formulation and level set method", Image and vision computing, Vol. 28, No. 4, 2010, pp. 668-676.

[36] A. Chambolle, "An algorithm for total variation minimization and applications", Journal of mathematical imaging and vision, Vol. 20, No. (1-2), 2004, pp. 89-97.

[37] K. Zhang, H. Song, and L. Zhang, "Active contours driven by local image fitting energy", Pattern recognition, Vol. 43, No. 4, 2010, pp. 1199-1206.

Hui Wang received his B.S. degree in applied mathematics from Central South University, Changsha, Hunan, China, in 2007, and M.S. degree in applied mathematics from China Agricultural University, Beijing, China, in 2009, and Ph.D. degree from the University of Electronic Science and Technology of China, Chengdu, Sichuan, China, in 2014. He is an associate professor in School of Mathematics and Physics, Anshun University. His research interests include image processing and compressive sensing.

Yingqiong Du received her B.S. degree in prospecting technology and engineering from Changchun Institute of Technology, Changchun, Jilin, China, in 2012, and M.S. degree in geological engineering from Chengdu University of Technology, Chengdu, Sichuan, China, in 2015. She is a lecturer in School of Resources and Environment Project, Anshun University. Her research interests include remote sensing image processing.